

# Investigation of the velocity, mach number, and turbulent parameters for different projectile rear geometry

Mehmet Hanifi Doğru<sup>1\*</sup>, İbrahim Göv<sup>2</sup>

<sup>1</sup> Department of Pilotage, Gaziantep University, Gaziantep, Türkiye.

<sup>2</sup> Department of Aeronautics and Astronautics Engineering, Gaziantep University, Gaziantep, Türkiye.

**Orcid:** M.H. Doğru (0000-0001-6038-8308), İ. Göv (0000-0002-5513-0158)

**Abstract:** A firearm projectile consists of four main parts. The end part of the cartridge is called the bullet (core). When the weapon is fired, the bullet (core) shoots towards the target. In the literature, there are studies examining projectile geometries in terms of projectile velocity, range, and impact factor. By redesigning the geometric features, the velocity and turbulence states of the projectile can be improved. Therefore, in this study, a projectile with different rear geometries is analyzed in terms of velocity, turbulence energy, and Mach number. For projectile rear geometry, Sharp, 45-degree, and curve rear geometries are analyzed. After the analysis, parameters such as velocity, turbulent energy, and Mach number were analyzed. The results were then compared with each other and the most effective geometry was obtained.

**Keywords:** projectile, rear geometry, velocity, turbulent energy.

## 1. Introduction

Turbulence energy and velocity distribution are investigated for three different projectile tip shapes with different tip geometries. The maximum velocity drop according to the projectile tip geometry was determined. It has been determined which geometry causes the maximum velocity decrease [1].

Ballistic impact performance was investigated for the different tip types of bullets. Impact energy, deformation, and stress parameters were analyzed and compared to each other [2].

Christman and Gehring conducted an experimental study on the effect of phases on crater dimensions. Steel and aluminum rods with different aspect ratios were impacted into different target materials at different impact velocities [3].

In the study conducted by Shokrieh and Javadpour, a constant thickness armor was investigated. This armor consists of two layers, kevlar and ceramic based. LsDyna was used to obtain the ballistic velocity limit and the optimum armor thickness was determined [4].

The study was carried out by Lecysyn et. al. to analyze the situations that can occur when a high-velocity projectile

hits a tank filled with liquid. The authors focus on projectile target interactions and describe how the reduction of projectile velocity is related to the initial conditions of the target [5].

The boundary layer separation was investigated during flight time for supersonic bullets by Rausch et. al [6] and Srivastava [7]. The bullet flight stability was studied in terms of supersonic-boundary-layer separation.

A 155 mm standard bullet was utilized. For the aerodynamic-properties of the bullet, minimal wings were added to the bullet's shoulder to investigate the separation. Comparison and discussion were performed for the boundary layer structures and aerodynamic data by Ma et al [8].

The flow concept, which has induced shock, was investigated by Jiang et al [9] using a supersonic projectile traveling in tubes. This study is based on the investigation of numerical data obtained by Gupta et. al. when projectiles with different nose geometries impacted the target plate.

A pneumatic gun was used to shoot at different projectile velocities at different thicknesses of the target plate. At the end of the study, the effects of bullet nose geometry on the velocity and deformation of the target plate were obtained. With this information, the thickness of the plate was tried to be estimated. [10]

\* Corresponding author.  
Email: mhdogru@gantep.edu.tr



As a result of the literature review, it was determined that there are very few studies on the flow analysis of projectiles and almost no studies on the rear geometry of projectiles. Therefore, in this study, the effects of the rear geometries of the projectiles on the velocity, Mach number, and turbulence parameters of the projectile are investigated.

## 2. Methodology

The effect of the rear geometry of the projectile is investigated to compare turbulence energy, Mach number, and velocity distribution of the projectile. The study is performed by using different three rear shapes which are sharp, 45-degree, and Curve shapes as shown in Figure 1. For projectile geometry, a 50-caliber projectile is used. 500 m/s initial velocity is defined for the projectile [1].

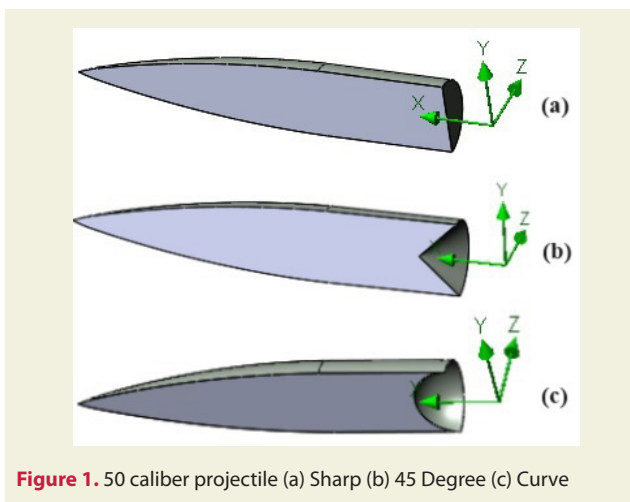


Figure 1. 50 caliber projectile (a) Sharp (b) 45 Degree (c) Curve

Turbulent energy, Mach number, and velocity of the projectile are achieved for each rear geometry at the end of the study.

Table 1. Dimensions of the flow domain

Axis	Dimension
X	0.5m
-X	0.3m
Y	0.15m
-Y	0.15m
Z	0.15m
-Z	0.15m

To perform this study, the SolidWorks flow simulation toolbox is used. The flow dimensions and view are given in Table 1 and Figure 2. For this flow analysis, external flow is used. In the computational domain, the distance -X is considered long in order to investigate the continuation of the backflow in more detail.

SolidWorks flow toolbox can be used for turbulent and laminar flows. Lam and Bremhorst proposed damping functions by using a modified k-ε turbulence model [11]. This describes transitional flows, turbulent, and laminar

homogeneous fluids consisting of the following turbulence conservation laws as given in equations 1-6.

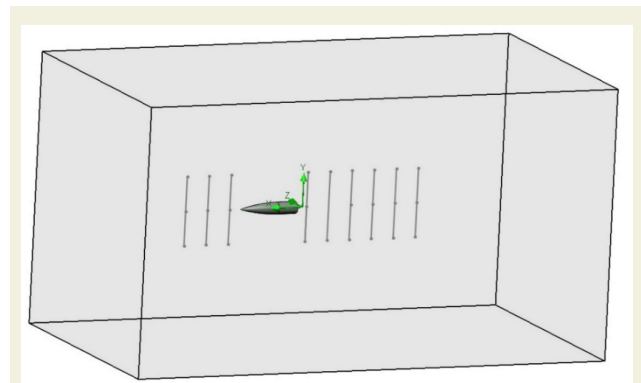


Figure 2. Flow domain view

$$\frac{\partial \rho k}{\partial t} + \frac{\partial \rho k u_i}{\partial x_i} = \frac{\partial}{\partial x_i} \left( \left( \mu + \frac{\mu_t}{\sigma_k} \right) \frac{\partial k}{\partial x_i} \right) + \tau_{ij}^R \frac{\partial u_i}{\partial x_j} - \rho \epsilon + \mu_t P_B \quad (1)$$

$$\frac{\partial \rho \epsilon}{\partial t} + \frac{\partial \rho \epsilon u_i}{\partial x_i} = \frac{\partial}{\partial x_i} \left( \left( \mu + \frac{\mu_t}{\sigma_\epsilon} \right) \frac{\partial \epsilon}{\partial x_i} \right) + C_{\epsilon 1} \frac{\epsilon}{k} \left( \tau_{ij}^R \frac{\partial u_i}{\partial x_j} + C_B \mu_t P_B \right) - f_2 C_{\epsilon 2} \quad (2)$$

$$\tau_{ij} = S_{ij} \quad (3)$$

$$\tau_{ij}^R = \mu_t S_{ij} - \frac{2}{3} \rho k \delta_{ij} \quad (4)$$

$$S_{ij} = \frac{\partial u_i}{\partial x_j} + \frac{\partial u_j}{\partial x_i} - \frac{2}{3} \delta_{ij} \frac{\partial u_k}{\partial x_k} \quad (5)$$

$$P_B = - \frac{g_i}{\sigma_B} \frac{1}{\rho} \frac{\partial \rho}{\partial x_i} \quad (6)$$

The mesh structure is created by using the unstructured mesh method as given in Figure 3. The optimum element number is obtained as 450000 elements according to the mesh accuracy study.

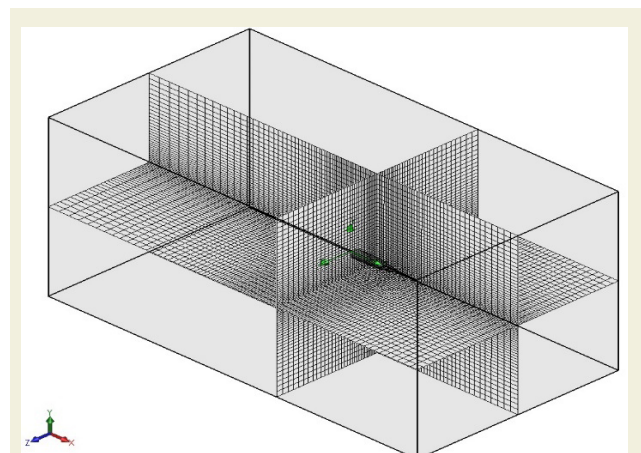


Figure 3. Mesh view of projectile

In the analysis, measurements were taken from different distances of the projectile within the computational domain as shown in Figure 4. In these measurements, velocity, Mach number, and turbulence parameters were obtained and information about the state of the flow was tried to be obtained.

Measurements were taken at  $-5D$ ,  $-3D$ , and  $-D$  distances to determine whether there was any flow variation in the distance in front of the projectile tip.

### 3. Results and Discussions

#### 3.1. Sharp Type Rear

Sharp-type rear geometry is analyzed in terms of the velocity distribution as given in Figure 5. The geometric information of the projectile is used as length is 64.63 mm and diameter is 13 mm for the projectile. 500 m/s initial velocity is defined for the projectile.

Figure 6 shows that the maximum velocity decrease is obtained at nearly 28 m/s in  $D$  measure after the rear of the projectile. It is observed that the speed decrease gradually decreases with increasing distance  $D$ .

Mach number is calculated according to the velocity of the projectile as nearly 1.45. Figure 7 and Figure 8 show that the maximum Mach number decrease is found as 0.087 in  $D$  measure after the rear of the projectile.

Mach number distribution is given in Figure 8 for all  $D$  measures.

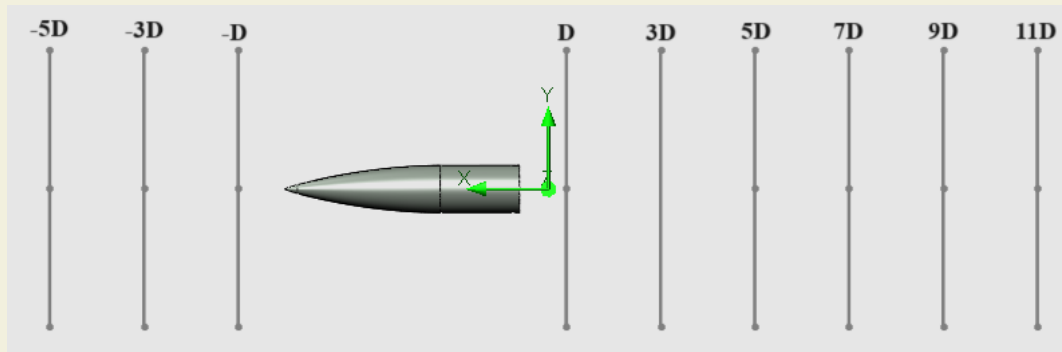


Figure 4. Measurement location for flow in the computational domain

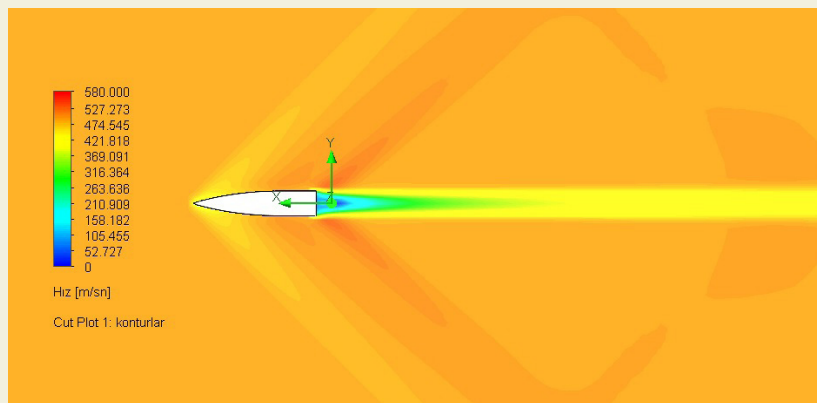


Figure 5. Sharp projectile velocity

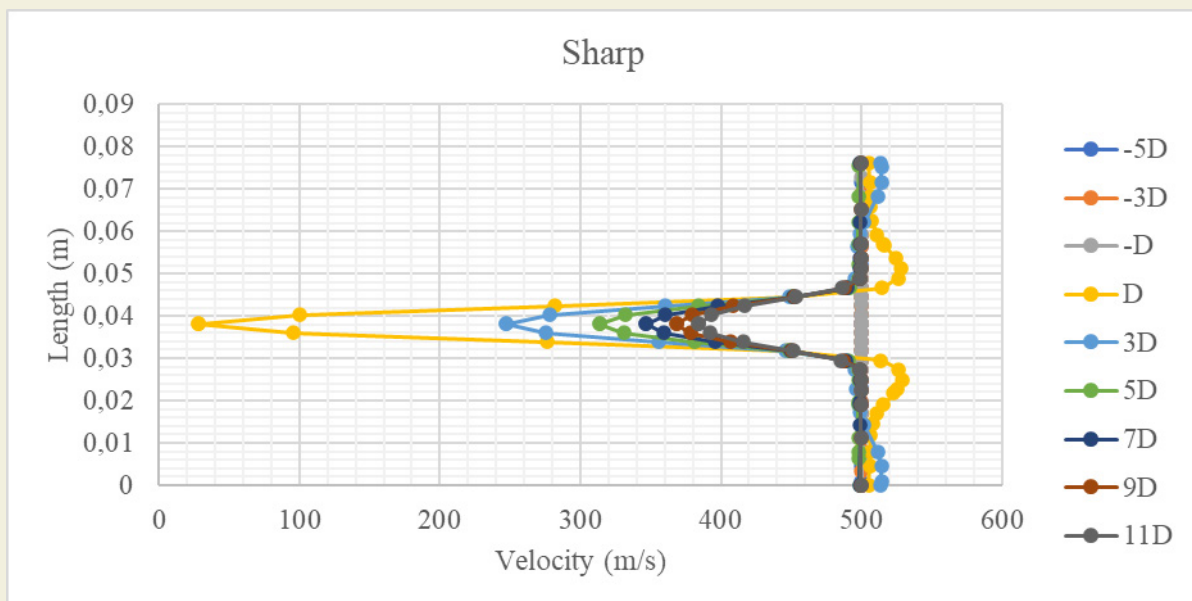


Figure 6. Sharp projectile velocity distribution according to  $D$  measure

Turbulent energy can be defined as the amount of energy per unit mass. Turbulent energy distribution on the projectile is given in Figure 9.

According to the geometric properties, the increment of the turbulent energy is found as 7599 J/kg for the sharp type of projectile on D measure as given in Figure 10.

### 3.2. 45 Degree Rear Type

45-degree type rear geometry is analyzed in terms of the velocity distribution as given in Figure 11. 500 m/s initial velocity is defined for the projectile. In the analyses performed, the most appropriate geometry between sharp and curve is considered to be 45 degrees and this geometry was used for comparison.

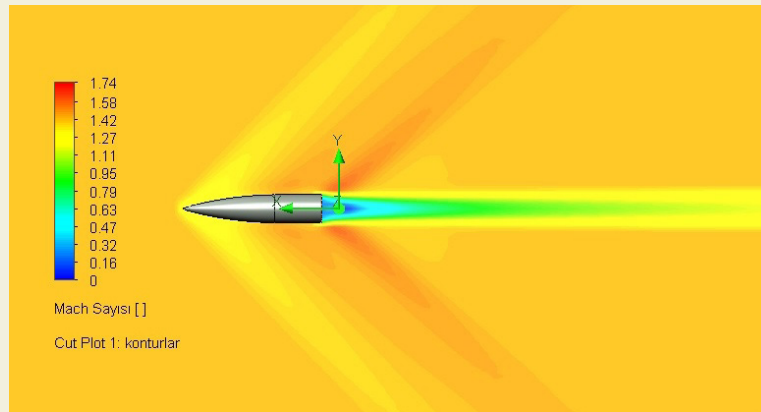


Figure 7. Sharp projectile Mach number

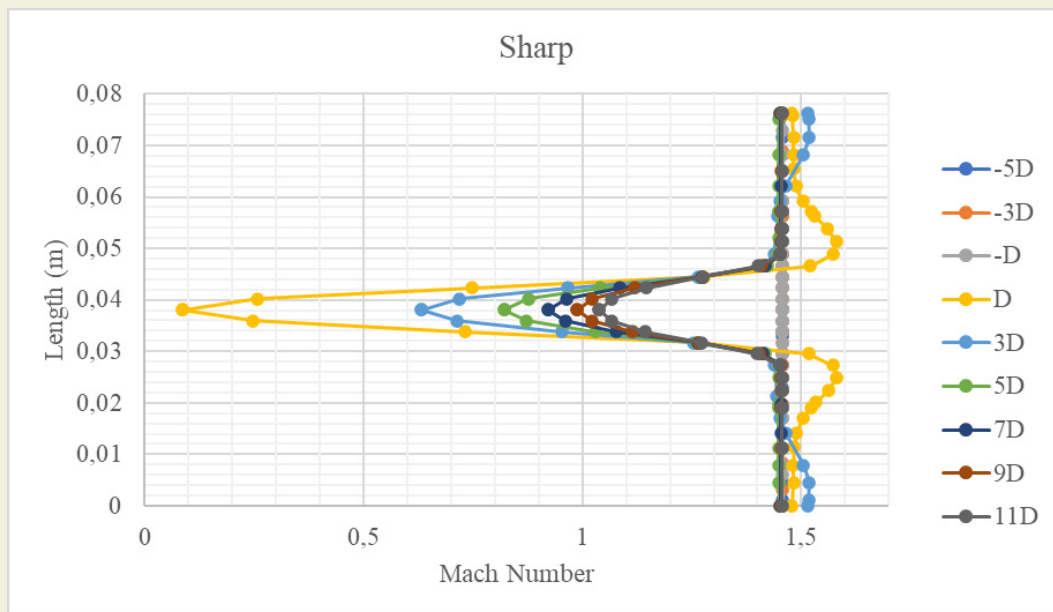


Figure 8. Sharp projectile Mach number distribution according to D measure

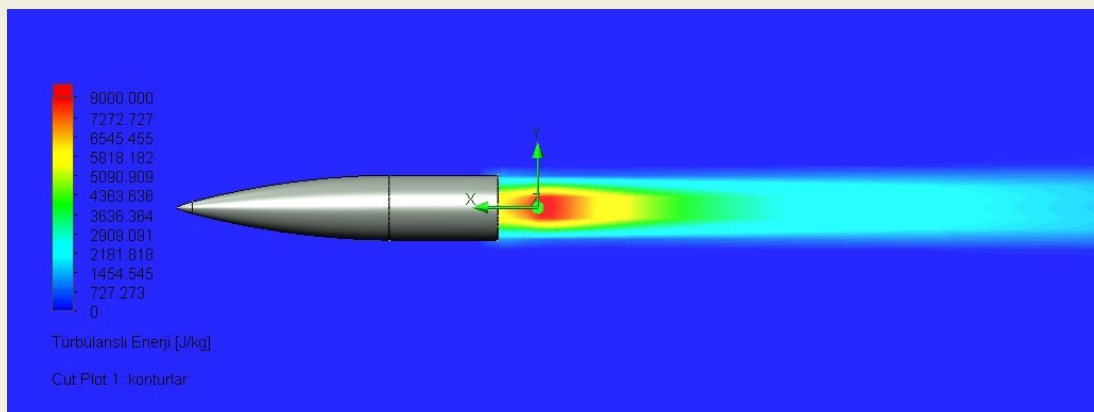


Figure 9. Sharp projectile turbulent energy

Figure 12 shows that the maximum velocity decrease is obtained at nearly 26 m/s in D measure after the rear of the 45-degree projectile. It is observed that the speed de-

crease gradually decreases with increasing distance D.

Figure 13 and Figure 14 show that the maximum Mach

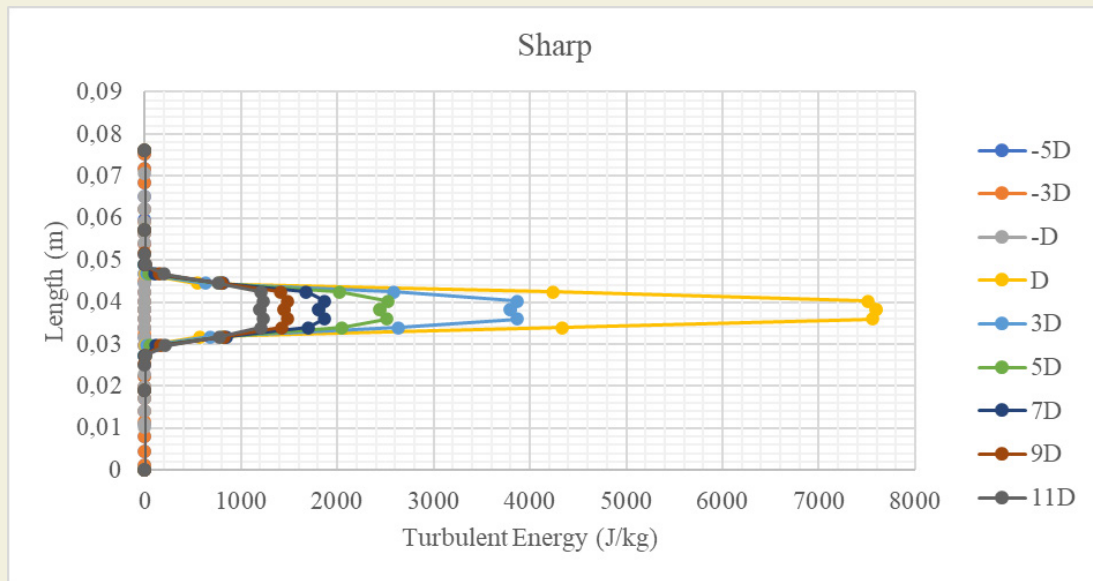


Figure 10. Sharp projectile turbulent energy distribution according to D measure

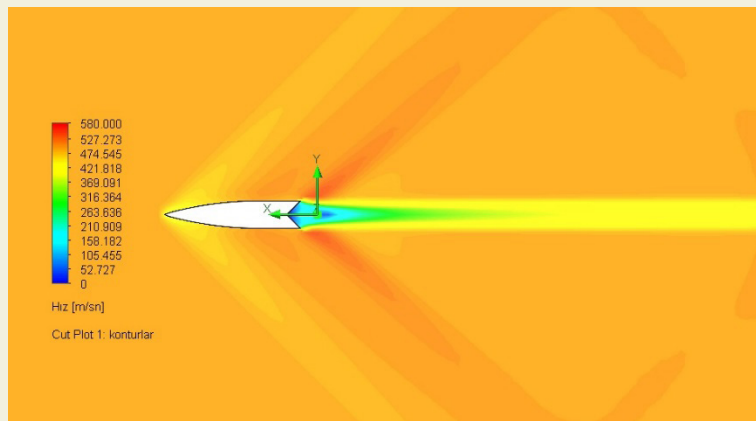


Figure 11. 45 Degree projectile velocity

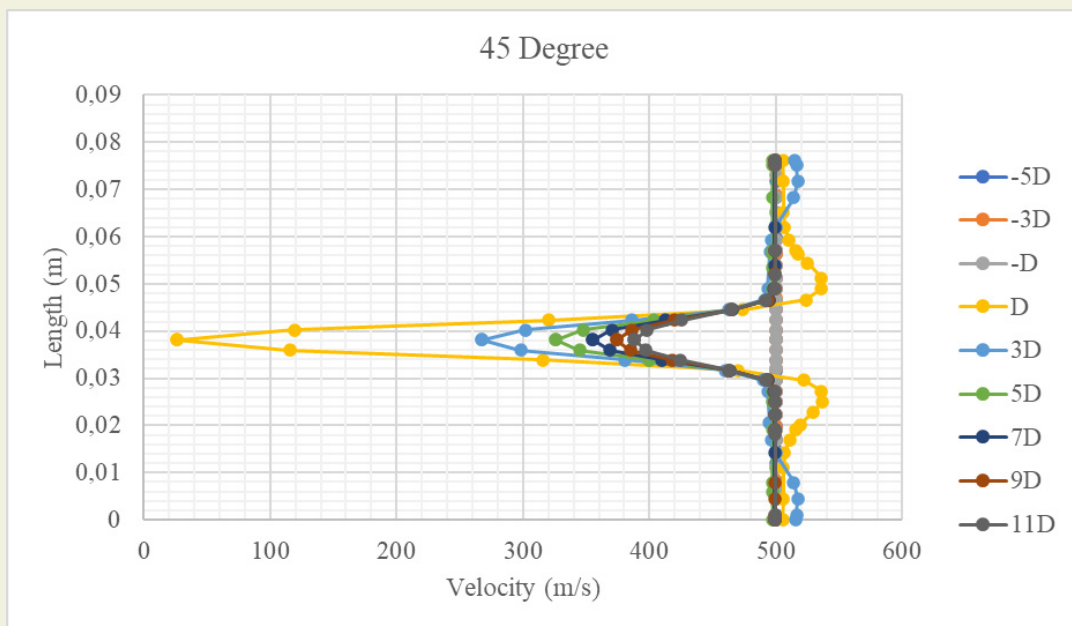


Figure 12. 45 Degree projectile velocity distribution according to D measure

number decrease is found as 0.098 in D measure after the rear of the 45 Degree projectile.

Mach number distribution is given for 45 Degree projectile in Figure 14 for all D measures.

Turbulent energy distribution on 45 Degree projectile is given in Figure 15. According to the geometric properties, the increment of the turbulent energy is found as 7643 J/kg for 45 45-degree type of projectile on D measure as given in Figure 16.

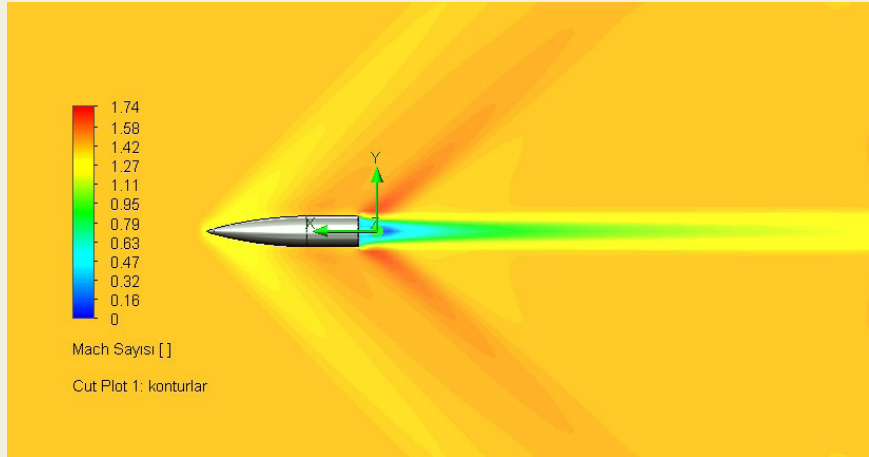


Figure 13. 45 Degree projectile Mach number

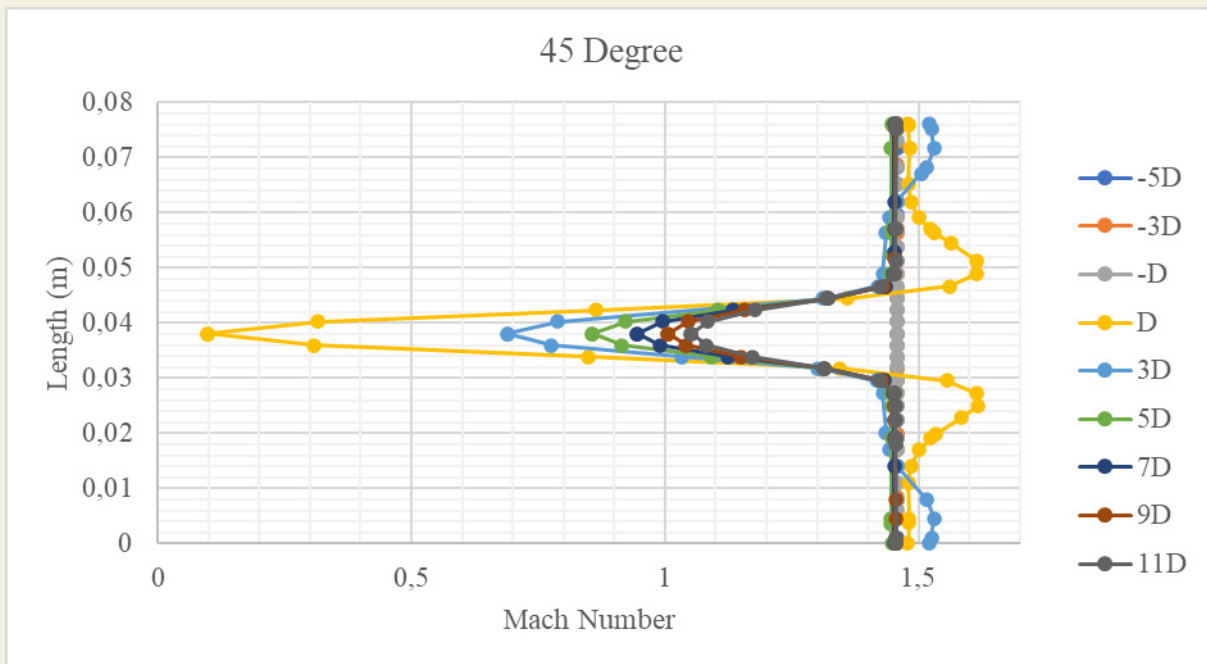


Figure 14. 45 Degree projectile Mach number distribution according to D measure

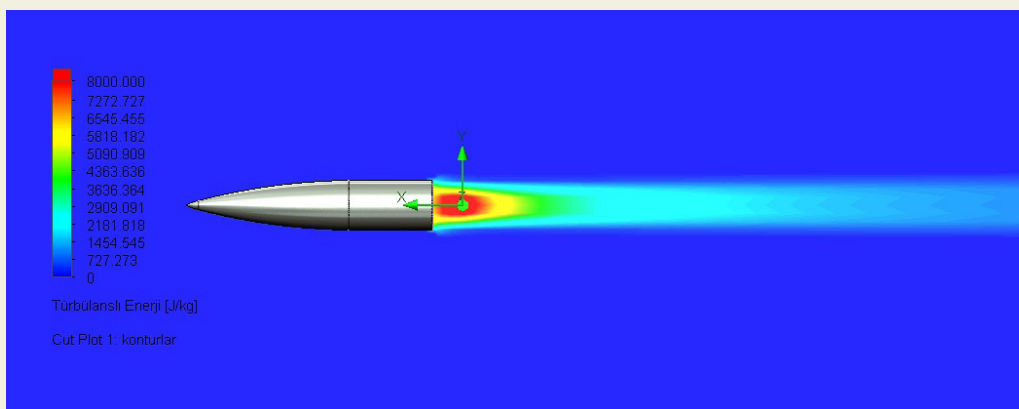


Figure 15. 45 Degree projectile turbulent energy

### 3.3. Curve Rear Type

Curve-type rear geometry is analyzed in terms of the velocity distribution as given in Figure 17. 500 m/s initial velocity is defined for the projectile.

Figure 18 shows that the maximum velocity decrease is obtained at nearly 45 m/s in D measure after the rear of the curve projectile. It is observed that the speed decrease gradually decreases with increasing distance D.

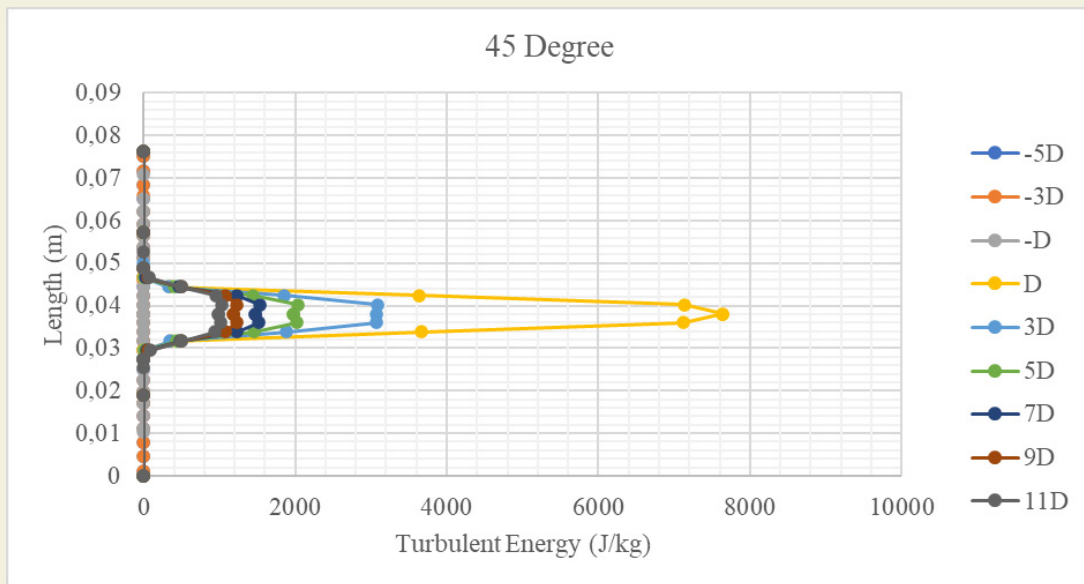


Figure 16. 45 Degree projectile turbulent energy distribution according to D measure

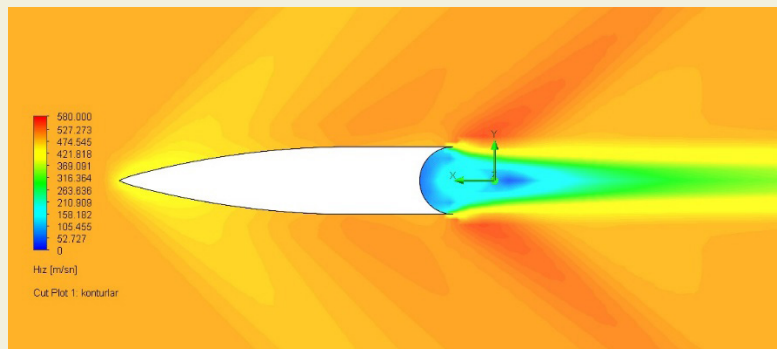


Figure 17. Curve projectile velocity

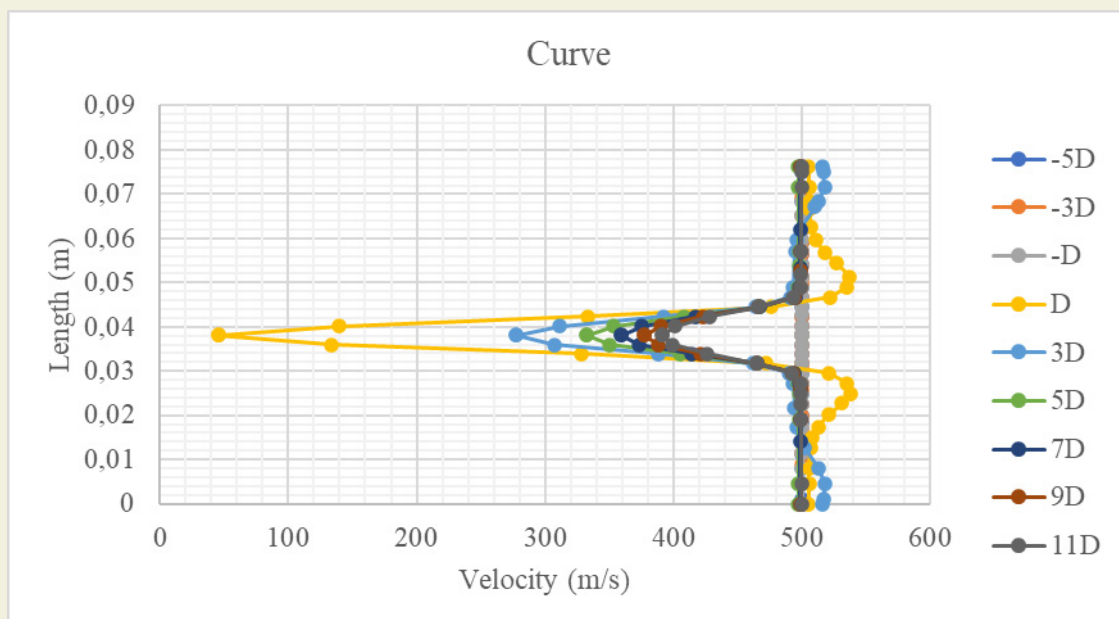


Figure 18. Curve projectile velocity distribution according to D measure

Mach number distribution of curve type projectile is given in Figure 20 for all D measures.

Figure 19 and Figure 20 show that the maximum Mach number decrease is found as 0.133 in D measure after the rear of the curve type projectile.

Turbulent energy distribution on the curve projectile is given in Figure 21.

According to the geometric properties, the increment of the turbulent energy is found as 7936 J/kg for the curve type of projectile on D measure as given in Figure 22.

### 4. Conclusions

In this study, a projectile with different rear geometries is analyzed in terms of velocity, turbulence energy, and Mach number. For projectile rear geometry, Sharp,

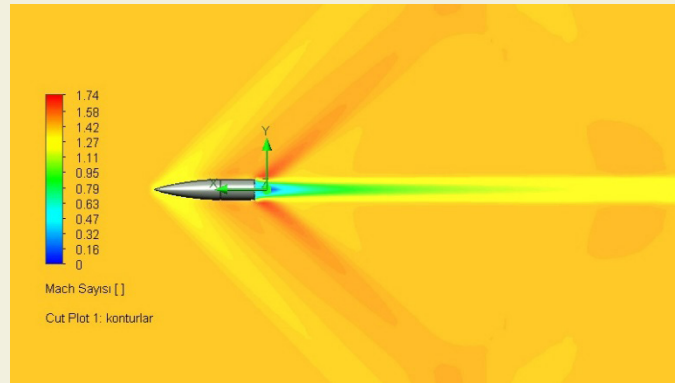


Figure 19. Curve projectile Mach number

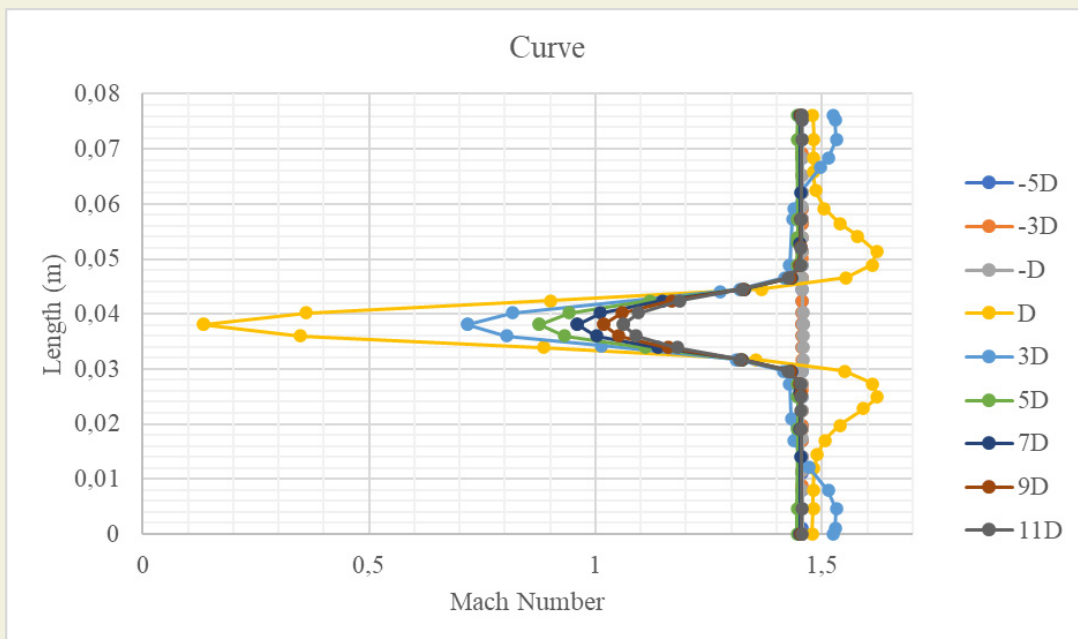


Figure 20. Curve projectile Mach number distribution according to D measure

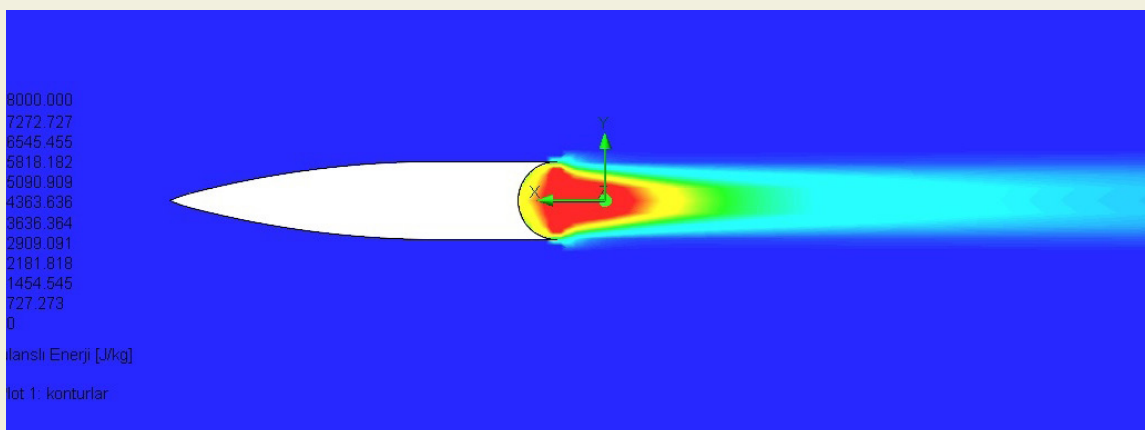


Figure 21. Curve projectile turbulent energy

45-degree, and curve rear geometries are analyzed. After the analysis, parameters such as velocity, turbulent energy, and Mach number were analyzed.

Minimum velocity, minimum Mach number, and maximum turbulent energy values are obtained according to change in D for sharp type projectile as given in Table 2.

Since it was found that there were no significant changes in the measurements taken at the rear of the bullet after the 11D distance, the measurements taken after the 11D distance were not included in the study.

Minimum velocity, minimum Mach number, and maximum turbulent energy values are obtained according to change in D for 45 Degree type projectile as given in Table 3.

Minimum velocity, minimum Mach number, and maxi-

imum turbulent energy values are obtained according to change in D for curve type projectile as given in Table 4.

As a result of the measurements taken at different D distances, it was determined that the maximum speed decrease was at D distance. When a comparison is made according to different back geometries (Figure 23), the velocity decrease obtained in the 45-degree projectile is 42% compared to the curve projectile, and the velocity decrease in the sharp projectile is 38% compared to the curve projectile.

As a result of the measurements taken at different D distances, it was determined that the maximum Mach number decrease was at D distance. When a comparison is made according to different back geometries (Figure 24), the Mach number decrease obtained in the 45-degree projectile is 26% compared to the curve projectile and

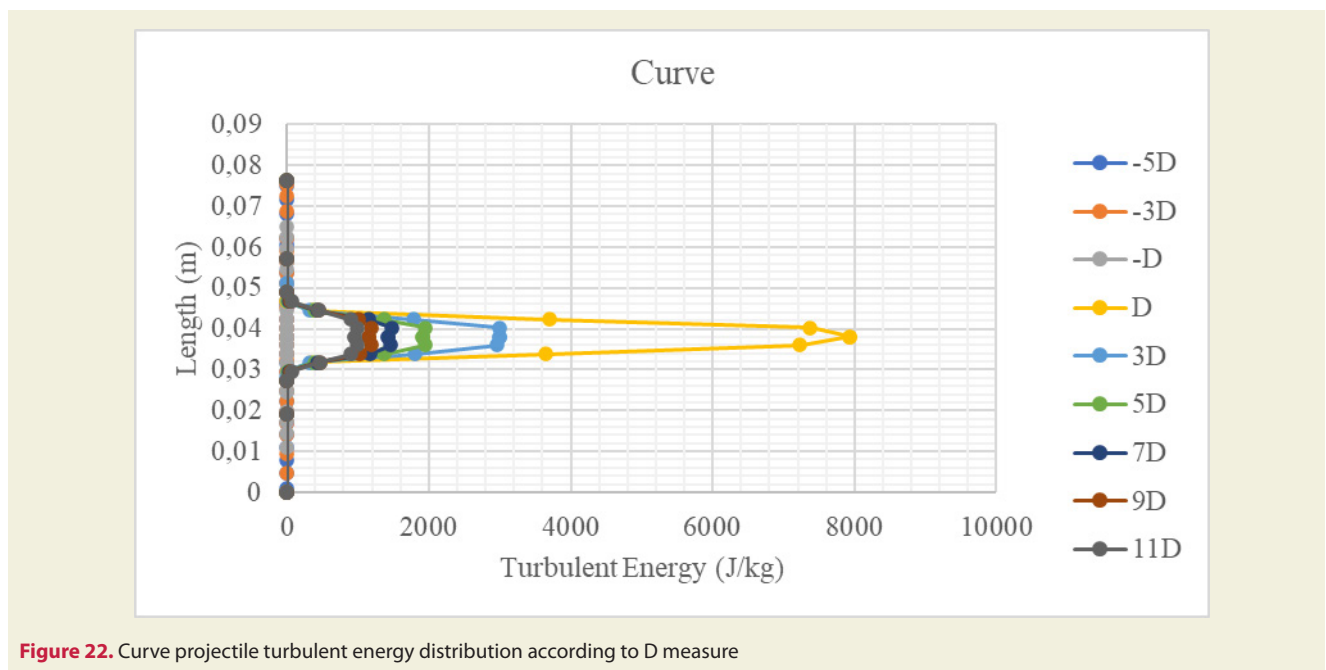


Figure 22. Curve projectile turbulent energy distribution according to D measure

Table 2. Sharp-type projectile aerodynamic parameters according to change in D

Shap Projectile Type	-5D	-3D	-D	D	3D	5D	7D	9D	11D
Min Velocity	500	500	499.97	28.49	247	313	346	368	384
Min Mach Number	1.457	1.457	1.456	0.087	0.632	0.821	0.922	0.986	1.039
Max Turbulent Energy	0.319	0.308	0.298	7599	3869	2519	1872	1488	1232

Table 3. 45 Degree type projectile aerodynamic parameters according to change in D

45 Degree Projectile Type	-5D	-3D	-D	D	3D	5D	7D	9D	11D
Min Velocity	500	500	499.97	26.62	267	325	354	373	388
Min Mach Number	1.457	1.457	1.456	0.098	0.688	0.857	0.946	1.01	1.051
Max Turbulent Energy	0.319	0.308	0.298	7643	3079	2030	1531	1233	1031

Table 4. Curve type projectile aerodynamic parameters according to change in D

Curve Projectile Type	-5D	-3D	-D	D	3D	5D	7D	9D	11D
Min Velocity	500	500	499.97	45.49	277	332	359	377	391
Min Mach Number	1.457	1.457	1.456	0.133	0.717	0.877	0.960	1.02	1.061
Max Turbulent Energy	0.319	0.308	0.298	7936	3002	1952	1470	1184	989

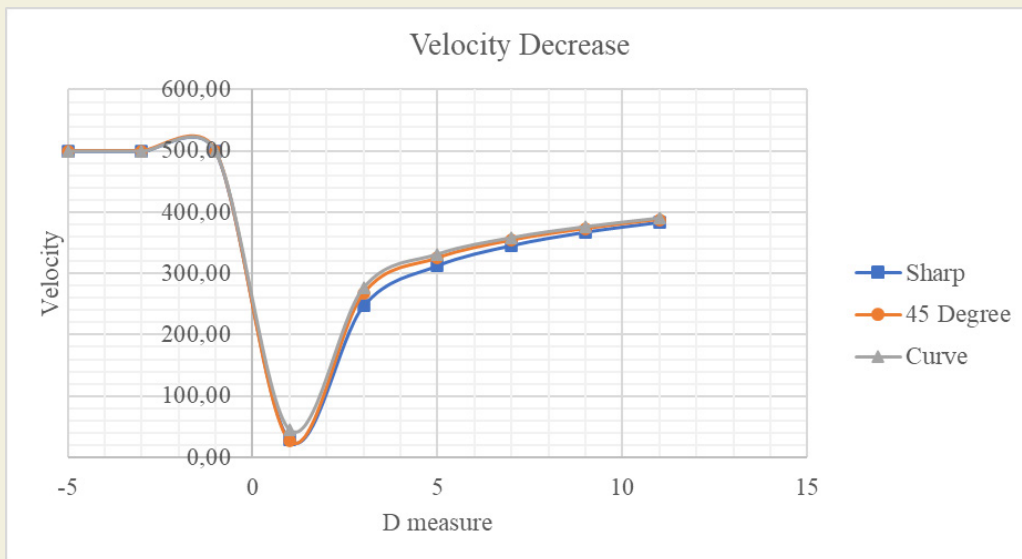


Figure 23. Comparison velocity decrease for different type of projectile

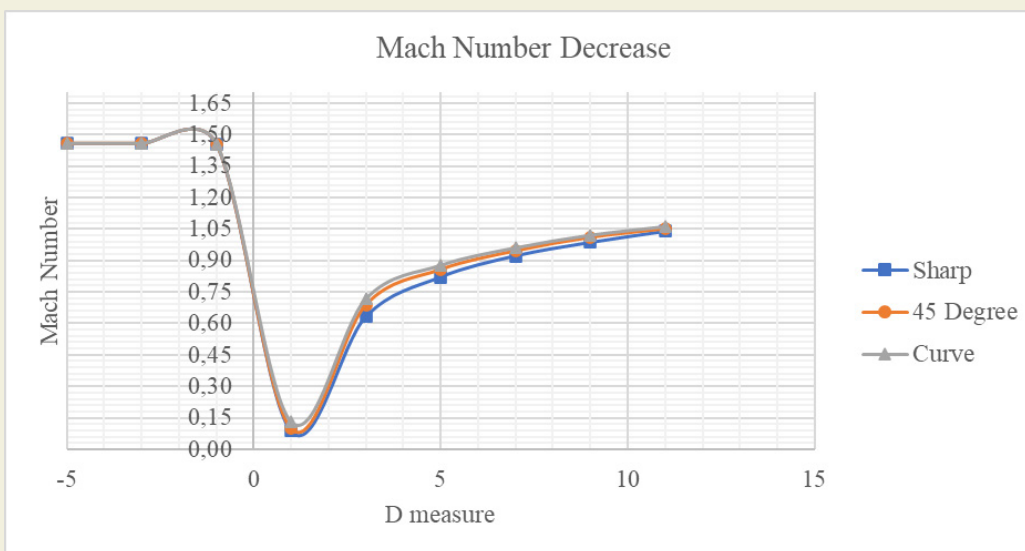


Figure 24. Comparison Mach number decrease for different types of projectiles

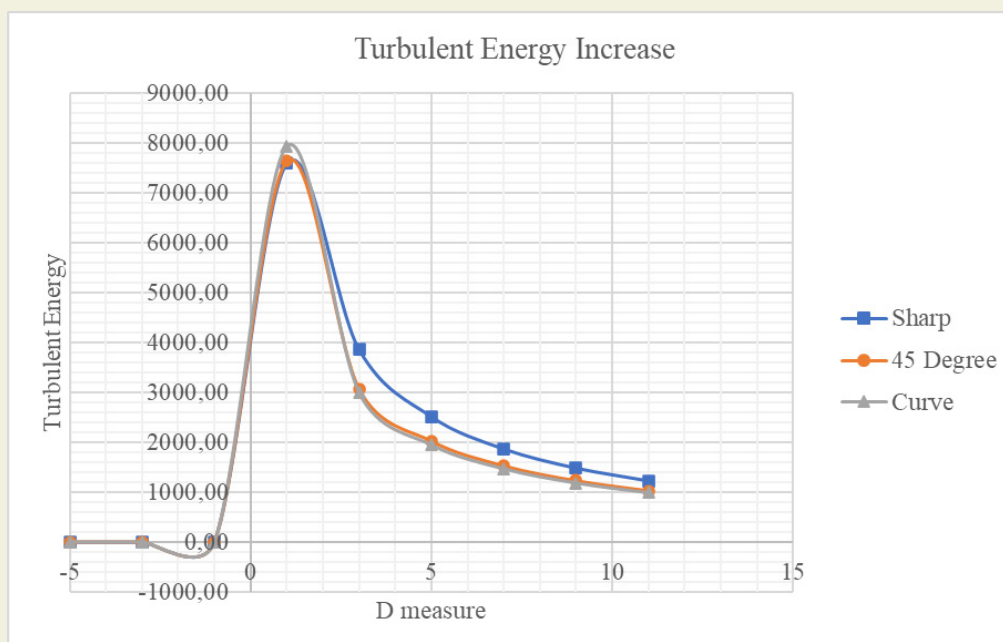


Figure 25. Comparison turbulent energy increase for different types of projectile

the Mach number decrease in the sharp projectile is 34%

As a result of the measurements taken at different D distances, it was determined that the turbulence energy was highest at D distance. When a comparison was made according to different back geometries, it was determined that the most intense turbulence energy occurred in the

compared to the curve projectile.

curve projectile with 7936 J/kg. The turbulence intensity obtained in the curve projectile was 3.7% higher than the 45-degree projectile and 4.2% higher than the sharp projectile as shown in Figure 25.

## References

- [1] Dođru, M. H. (2017). Investigation of Velocity Distribution and Turbulent Energy for the Different Tip Shaped Projectiles. *Çukurova University Journal of the Faculty of Engineering and Architecture*, 32(3), 39-46. DOI: 10.21605/cukurovaumfd.357183
- [2] Subaşı, M., Dođru, M. H., Yeter, E., & Yılmaz, N. F. (2020). Investigation of The Bullet Impact Energy Performance According to Variable Tip Geometry. *The International Journal of Materials and Engineering Technology*, 3(1), 10-15.
- [3] Christman, D. R., & Gehring, J. W. (1966). Analysis of high-velocity projectile penetration mechanics. *Journal of Applied Physics*, 37(4), 1579-1587. DOI: 10.1063/1.1708570
- [4] Shokrieh, M. M., & Javadpour, G. H. (2008). Penetration analysis of a projectile in ceramic composite armor. *Composite structures*, 82(2), 269-276. DOI: 10.1016/j.compstruct.2007.01.023
- [5] Lecysyn, N., Dandrieux, A., Heymes, F., Slangen, P., Munier, L., Lapebie, E., ... & Dusserre, G. (2008). Preliminary study of ballistic impact on an industrial tank: Projectile velocity decay. *Journal of Loss Prevention in the Process Industries*, 21(6), 627-634. DOI: 10.1016/j.jlp.2008.06.006
- [6] Rausch J., Roberts B. (1975). Reaction Control System Aerodynamic Interaction Effects on Space Shuttle Orbiter, *Journal of Spacecraft and Rockets*, 12, 660-666. DOI: 10.2514/3.57032
- [7] Srivastava B. (1998). Aerodynamic Performance of Supersonic Missile Body-and Wing Tip-Mounted Lateral Jets, *Journal of Spacecraft and Rockets*, 35, 278-286. DOI: 10.2514/2.3352
- [8] Ma J., Chen Z-h., Huang Z-g., Gao J-g., Zhao Q. (2016). Investigation on the Flow Control of Micro-Vanes on a Supersonic Spinning Projectile, *Defence Technology*, 12, 227-233. DOI: 10.1016/j.dt.2016.01.008
- [9] Jiang Z, Huang Y, Takayama K. (2004). Shocked Flows Induced by Supersonic Projectiles Moving in Tubes, *Computers & fluids*, 33, 953-966. DOI: 10.1016/S0045-7930(03)00041-0
- [10] Gupta, N. K., Iqbal, M. A., & Sekhon, G. S. (2007). Effect of projectile nose shape, impact velocity and target thickness on deformation behavior of aluminum plates. *International Journal of Solids and Structures*, 44(10), 3411-3439. DOI: 10.1016/j.ijsolstr.2006.09.034
- [11] Lam, C.K.G. and Bremhorst, K.A. (1981). Modified Form of Model for Predicting Wall Turbulence, *ASME Journal of Fluids Engineering*, Vol.103, pp. 456-460. DOI: 10.1115/1.3240815